A Study of the Mountain Torque and its Interannual Variations in the Northern Hemisphere

ABRAHAM H. OORT AND HAROLD D. BOWMAN II[1]

Geophysical Fluid Dynamics Laboratory/NOAA, Princeton University, Princeton, N. J. 08540

(Manuscript received 6 March 1974, in revised form 2 July 1974)

ABSTRACT

Values of the large-scale mountain torque between 10S and 80N are computed for each month of the five-year period, May 1958 through April 1963. A careful comparison with earlier midseason values presented by Newton using different data sources and different analysis techniques is made. The calculations appear to be equally sensitive to differences in smoothing of the mountain profiles as to differences in basic geopotential height data used. Interannual variations in the monthly-mean mountain torques are found to be large, especially during the winter half-year.

In general, the large-scale mountain torque gives only a minor contribution to the total surface torque as estimated by other investigators. However, when integrated over the Northern Hemisphere as a whole, the mountain and frictional torques appear to be equally important. Both torques seem to act as a sink of angular momentum in summer and a source in winter.

1. Introduction

The role of mountains in the general scheme of the atmospheric circulation has recently been analyzed in some detail in several numerical simulation experiments. In these model experiments as described by Kasahara *et al.* (1973) mainly for the stratosphere and by Manabe and Terpstra (1974) in more depth for the global circulation, the January climate was simulated with the present land-sea distribution. Two cases were considered, one with realistic mountains and the other without any mountains. The comparison between the results from such sets of otherwise identical runs has provided valuable insight into the qualitative effects of mountains, such as in the redistribution between transient and stationary wave kinetic energy.

One of the important effects of mountains is the drag (or possibly push) exerted by them on the atmospheric flow. This effect can be discussed probably best from the viewpoint of the angular momentum balance as first suggested by Starr (1948) and later evaluated from real atmospheric data by White (1949), Widger (1949), and most recently by Newton (1971a). In these studies, the mountain torque was shown to be smaller than the frictional torque but not negligible, and generally to act in the same direction, that is, as a drag on the atmospheric flow. Since the numerical experiments described earlier begin to approach a realistic simulation of the atmosphere, it becomes more and more important to supply from observations accurate values for sensitive parameters describing the climate. Some of these parameters are the frictional and mountain torques.

In the first evaluation of the mountain torque, White (1949) used climatological-mean pressure data from the 1930's in the latitude belt between 25 and 65N. With more extensive recent pressure data, Newton (1971a) was able to extend the earlier analysis to cover all major mountain ranges on the globe for the midseason months. The agreement with White's results proved to be surprisingly good. In the present paper, the principal aim is to estimate for each month of the year the range of the year-to-year variations in the mountain torque over the Northern Hemisphere. It is of much interest to evaluate this range since it gives a measure of the representativeness of data from one particular year for the longer-term climatic mean value, and thus provides a valuable parameter to test the outcome of numerical experiments. Moreover, because of considerable uncertainty as to the best method of analysis, it will be useful to compare our five-year mean torques based on an objective analysis scheme with those given by Newton based on hand analysis.

The net torque exerted by the earth's surface on the atmosphere can, as was discussed before, be broken down into two components, one due to mountains and the other due to small-scale frictional effects. However, the breakdown is not unique at least from the observational point of view. The presently available network of meteorological stations can only

[1] Present affiliation: National Environmental Satellite Service/NOAA, Washington, D. C. 20031.

supply the large-scale features of the pressure fields in the free atmosphere with a resolution of at best about 5° latitude. This limitation means, of course, that the computed mountain torques contain only the large-scale effects of mountain ranges. The east-west pressure differences across the unresolved mountains [the "hill" torque (Lorenz, 1951)] are then often lumped together with the real friction effects. In numerical model experiments with their finite mesh, similar ambiguities arise. Unfortunately, there is, up to now, no conclusive evidence, either observational or theoretical, that large-scale effects dominate in the true mountain torque. Thus, the present torque values might change appreciably if one would include the finer details at a scale below a few hundred kilometers. In this context, the work, for example, by Bretherton (1969) and Lilly (1972) may be mentioned. These investigators find that under certain conditions mesoscale mountain features may have an important influence on the large-scale flow in the free atmosphere. By and large, the presently measured mountain torques seem to be determined by differences in the large-scale thermal structure of the atmosphere at the west and east sides of the major mountain ranges.

2. Formulation of the problem: Basic data and analysis technique

In the present study, the angular momentum balance will be formulated from the atmospheric viewpoint and not from that of the solid earth. In other words, a torque that contributes to an acceleration of the eastward flow will be counted as a positive contribution, and *vice versa*.

The general balance equation for eastward angular momentum in a (x,y,p) coordinate system relative to the rotating earth may be written in the form

$$\partial M/\partial t = -\nabla_3 \cdot M\mathbf{c} - g(\partial Z/\partial x)a\cos\phi + F_x a\cos\phi, \quad (1)$$

where

- a mean radius of earth
- $\mathbf{c}$ three-dimensional velocity vector in (x,y,p) coordinate system $[=(u,v,\omega)]$
- dx $a\cos\phi d\lambda$
- dy $ad\phi$
- F_x frictional force in x direction
- g acceleration due to gravity
- M absolute angular momentum per unit mass $[=(u+\Omega a\cos\phi)a\cos\phi]$
- t time
- Z geopotential height of an isobaric surface
- ∇_3 three-dimensional del-operator
- λ, ϕ longitude, latitude
- Ω angular speed of the earth's rotation.

According to Eq. (1), the angular momentum for a unit of mass may change due to (i) the local convergence of absolute angular momentum, (ii) a pressure torque, and (iii) a frictional torque. The present paper deals mainly with the second term. When one integrates this term horizontally along a latitude circle where not intersected by mountains (indicated by $\oint d\lambda$) and vertically from sea level (at pressure p_0) up to the top of the highest mountain range (at pressure p_T) along the latitude, one obtains the mountain torque $T_M(\phi)$:

$$T_M(\phi) = -\int_{p_T}^{p_0} \oint g(\partial Z/\partial\lambda)a\cos\phi d\lambda dp/g, \quad (2a)$$

or

$$T_M(\phi) = +\int_{p_T}^{p_0} \sum_i (Z_E^i - Z_W^i)a\cos\phi dp \quad (2b)$$

where the superscript i indicates the ith mountain range intersecting the integration path in the x direction at the pressure p, and the subscripts E and W indicate the east and west sides of the mountain range, respectively.

The geopotential height data needed in the present study were extracted from the MIT General Circulation Library. This Library contains daily radiosonde data taken at 0000 GMT for the five-year period, May 1958 through April 1963. All data in the sample of about 600 stations were checked on possible code errors and hydrostatic consistency. Many general circulation statistics were computed for each station

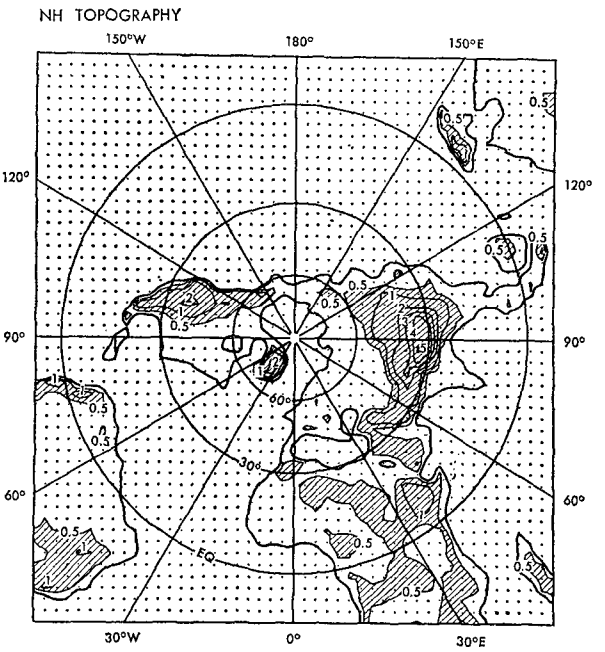

FIG. 1a. Network of grid points used in present study to analyze geopotential height fields. Resolution near 60N is about 500 km×500 km. Isopleths of topography are in thousands of meters.

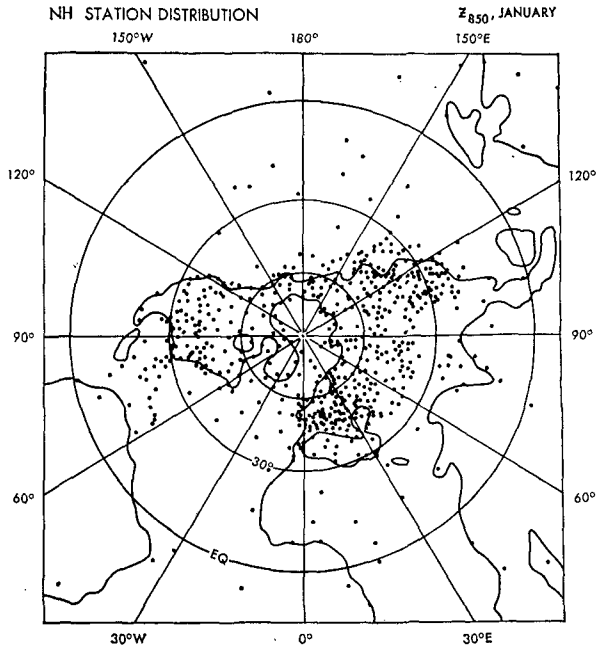

FIG. 1b. Distribution of radiosonde stations used in the present computations of the mountain torque for the month of January.

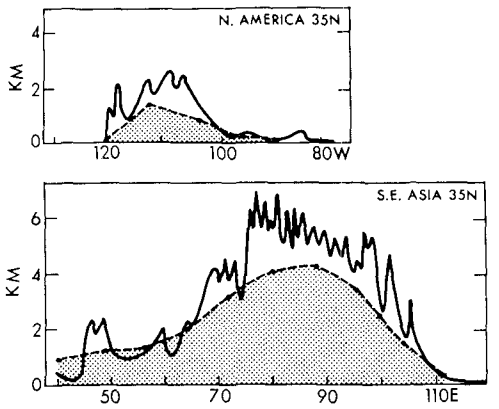

FIG. 2. Comparison of the topography used by Newton (solid curve) and by present authors (dashed curve, area under curve stippled) along 35N.

separately at the different levels, but of these parameters only the monthly-mean height values of the various isobaric surfaces are needed here. Following the station calculations, the data were then interpolated to a polar stereographic grid using an objective analysis scheme. The resolution of the analysis grid together with the topography is given in Fig. 1a, and may be compared with an example of the actual data distribution shown in Fig. 1b. Analyses were performed at the levels 1000, 950, 900, 850, 700, 500, 400, 300, 200, 100 and 50 mb. Of course, in the case of the mountain torque, only the first five or six levels contribute. The vertical integration in expression (2a) was carried out with 50-mb increments. For more detailed information on the data, data distribution

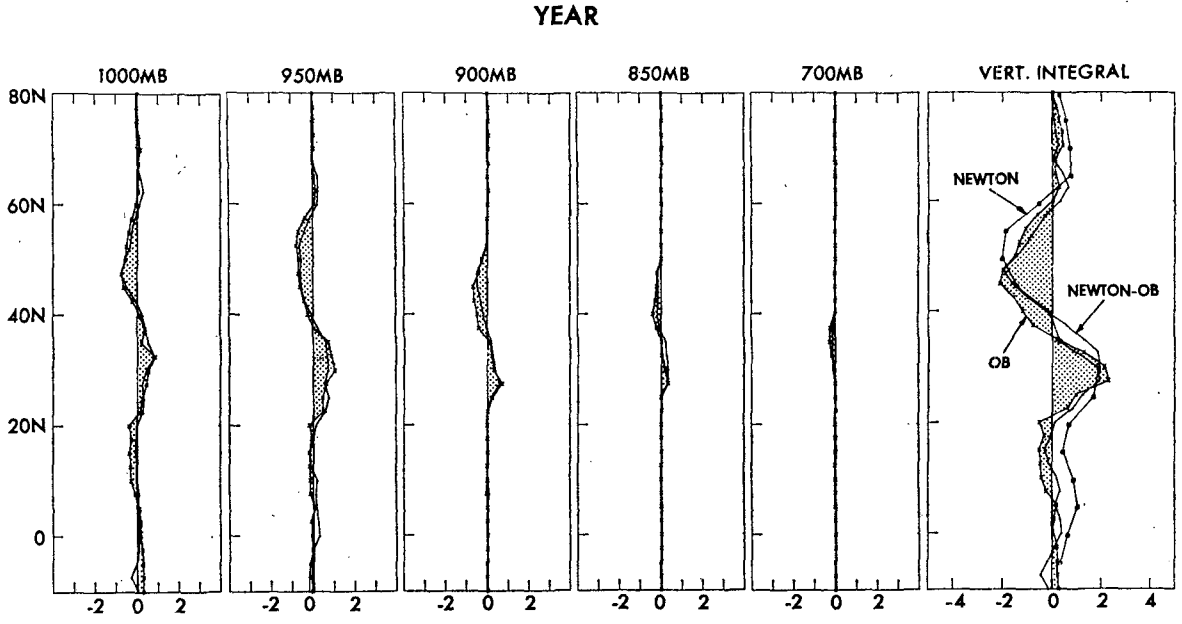

FIG. 3. Annual-mean contribution from different pressure levels to the mountain torque. Present results are shown by stippled area and curves labeled OB. The second set of curves shown by full lines without crosses or squares indicates the results obtained by using Newton's geopotential height fields, but our smoothed topography (labeled Newton-OB). The third curve on the right in the diagram of the vertical integrals (labeled Newton) indicates Newton's original results obtained by using his detailed topography. Units are in Hadleys $(37.5 \text{ mb})^{-1}$ at 1000 mb, in Hadleys $(50 \text{ mb})^{-1}$ at 950, 900, 850 and 700 mb, and in Hadleys for the vertical integral.

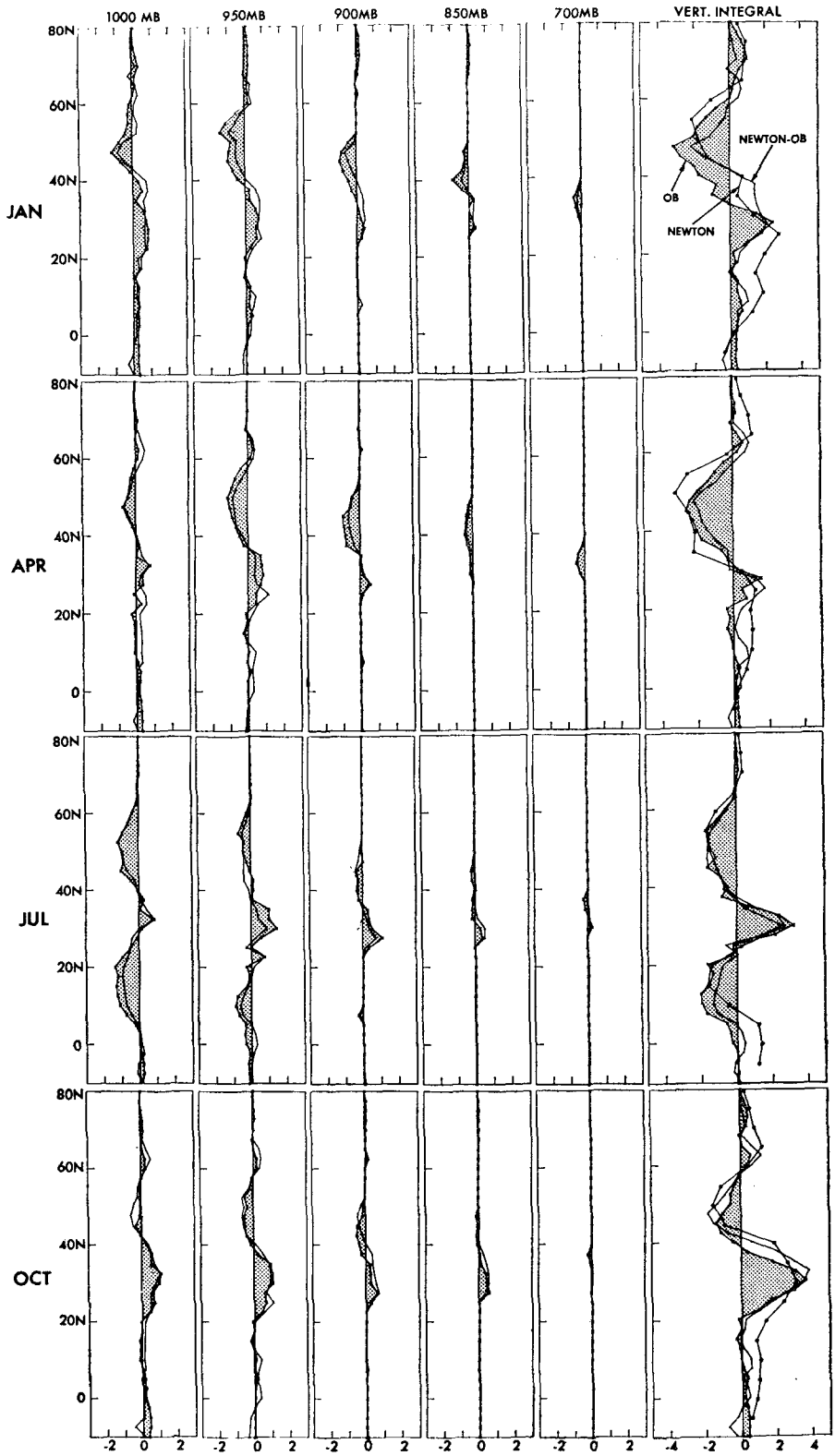

FIG. 4. Contribution from different pressure levels to the mountain torque for January, April, July and October (see legend to Fig. 3).

and analysis techniques, one is referred to a paper by Oort and Rasmusson (1971).

To obtain the necessary computational accuracy for the mountain torque, the basic height fields were interpolated from the original polar stereographic to a latitude-longitude grid, ranging in latitude between 15S and 80N, and in longitude between 176W and 176E. On this last grid in the case of no mountains, the sum of the finite geopotential height differences along a latitude circle, and thus also the mountain torque, will vanish exactly as they should. Because of computational convenience, the distance between grid points was chosen to be 8° in longitude and 2.5° in latitude. Therefore, only topographic features with an east-west scale of at least 8° longitude and a north-south scale of at least 2.5° latitude are included in the present computations.

The mountain heights, as derived from the basic Scripps topographical data, were interpolated to the same latitude-longitude grid to make the analysis of mountain topography compatible with the geopotential height analyses. Resulting mountain profiles at 35N are shown in Fig. 2 and compared with those adopted by Newton (1971a). In this study, Newton attempted to incorporate by hand analysis the smaller-scale features of the profiles, but using at the same time geopotential height fields that are only known at a much coarser scale. Further in the paper, the two methods will be discussed in more detail.

As a last point of possible significance, let us mention that the geopotential height analyses used here are based only on actual observed height data. Thus, for example, no wind data were used through the geostrophic or thermal wind relations to aid the analyses.

3. Normal annual cycle

The computed mountain torque and its vertical structure for the year and the four midseason months are shown in Figs. 3 and 4. For comparison, Newton's (1971a) results are added. The curves represent the values of the mountain torque as defined by (2b), but in addition, integrated meridionally over 5° latitude belts. The resulting integrals are expressed in Hadley units (1 Hadley$=10^{25}$ gm cm^2 sec^{-2}), which will be used throughout the paper. These units have been proposed first by Newton.

In Figs. 3 and 4, three different evaluations are shown to illustrate the uncertainty involved in the computation of the mountain torque. Shown are:

(i) The present torque values (stippled area delineated by curves labeled OB, with crosses).
(ii) The torque values computed by using Newton's geopotential height data as taken from Crutcher and Meserve (1970), our topography (resolution 8° in longitude and 2.5° in latitude), and our method of computation (curves labeled Newton-OB).
(iii) Newton's torque values as taken from his paper (curves labeled Newton, with squares).

The differences between cases (i) and (ii) can only be due to differences in the geopotential height data, between cases (ii) and (iii) only due to differences in topography and method of computation, and between cases (i) and (iii) due to both differences in geopotential height data and in topography and method of computation.

Thus, one would expect that the case (ii) curves would lie in between Newton's and the present results.

TABLE 1. Vertically integrated mountain torque (Hadleys)* for 5° latitude-wide belts and for the Northern Hemisphere, based on geopotential height data from May 1958 through April 1963.

	Latitudes																	
Month	10S	5S	0	5N	10N	15N	20N	25N	30N	35N	40N	45N	50N	55N	60N	65N	70N	75N	NH
Jan	0.2	0.2	0.3	0.7	0.4	0.1	0.1	1.9	2.1	0.3	−1.3	−2.6	−2.3	−1.3	0.1	0.4	1.2	0.8	1.5
Feb	0.2	0.2	0.3	0.7	0.2	0.0	−0.1	1.5	1.1	0.1	−0.6	−1.2	−1.5	−0.4	0.5	0.5	1.0	0.6	3.1
Mar	0.2	0.2	0.2	0.6	0.0	−0.1	−0.2	1.3	0.6	0.0	−0.5	−0.3	−0.4	−0.1	0.8	0.3	0.8	0.3	3.5
Apr	0.2	0.2	0.1	0.4	−0.1	−0.3	−0.4	0.6	0.3	0.1	−1.9	−2.5	−2.1	−1.1	0.4	0.2	0.3	0.1	−5.8
May	0.2	0.1	0.0	0.2	−0.7	−0.8	−0.7	0.8	0.8	−0.3	−1.8	−2.2	−2.1	−1.3	−0.1	0.4	0.6	0.4	−6.3
Jun	0.1	0.0	−0.2	−0.2	−1.4	−1.3	−1.3	−0.2	1.2	−0.5	−1.4	−2.1	−2.0	−1.5	−0.3	0.0	0.2	0.3	−10.5
Jul	0.1	0.1	−0.3	−0.3	−1.8	−1.5	−1.5	−0.3	2.6	0.2	−0.8	−1.6	−1.5	−1.5	−0.7	−0.1	0.1	0.2	−8.5
Aug	0.1	0.1	−0.3	−0.5	−1.8	−1.5	−1.8	−1.5	3.0	1.4	−0.1	−1.1	−1.2	−1.1	−0.3	0.2	0.3	0.3	−5.3
Sep	0.2	0.2	−0.1	−0.2	−1.2	−1.1	−1.0	0.2	3.8	2.4	0.4	−0.7	−1.2	−1.1	−0.1	0.0	0.7	0.4	1.4
Oct	0.3	0.3	0.2	0.4	−0.0	−0.3	−0.6	0.6	3.0	1.6	0.1	−0.5	−0.5	−0.1	0.5	0.1	0.5	0.4	5.5
Nov	0.3	0.3	0.3	0.5	0.4	0.1	0.1	1.9	1.6	0.5	−1.0	−2.0	−1.5	−1.0	0.2	0.1	0.3	0.3	0.9
Dec	0.2	0.2	0.3	0.7	0.6	0.2	0.1	1.7	1.6	0.2	−1.1	−2.5	−1.8	−0.4	0.8	0.4	0.6	0.4	2.2
Year	0.2	0.2	0.1	0.2	−0.5	−0.5	−0.6	0.7	1.8	0.5	−0.8	−1.7	−1.5	−0.9	0.2	0.2	0.5	0.4	−1.5
F**	13.8	14.1	14.2	14.1	13.8	13.3	12.5	11.7	10.7	9.5	8.3	7.1	5.9	4.7	3.6	2.5	1.7	1.0	63.8

* 1 Hadley$=10^{25}$ gm cm^2 sec^{-2}.
** To obtain the average stress due to mountains in units of dyn cm^{-2}, divide values by conversion factor F at appropriate latitude:

$$F=\int_{\phi-2.5}^{\phi+2.5} 2\pi a^3 \cos^2\phi \, d\phi.$$

TABLE 2. Vertically integrated mountain torque (Hadleys) for 5° latitude-wide belts and for the Northern Hemisphere for the 60 months from May 1958 through April 1963.

Month	Latitude 10S	0	10N	20N	30N	40N	50N	60N	70N	Northern Hemisphere
May 1958	−0.2	−0.1	−0.6	−0.7	0.6	−0.9	−1.8	−0.1	0.5	−5.6
Jun 1958	−0.1	−0.2	−1.4	−1.3	0.7	−0.3	−1.7	−0.7	0.4	−7.8
Jul 1958	−0.0	−0.3	−2.0	−1.7	2.4	−0.2	−1.0	−0.6	0.3	−4.0
Aug 1958	−0.2	−0.4	−1.9	−1.6	3.3	0.5	−0.6	−0.1	−0.2	−1.7
Sep 1958	−0.1	−0.2	−1.2	−1.2	4.1	1.0	−1.2	−0.1	1.0	3.3
Oct 1958	0.1	0.1	−0.1	−0.3	4.5	0.8	−0.7	0.7	0.3	10.2
Nov 1958	0.1	0.3	0.8	0.3	2.2	−1.1	−2.7	−0.0	0.8	2.8
Dec 1958	0.1	0.3	0.7	0.1	1.0	−0.4	−1.1	1.3	1.1	7.1
Jan 1959	0.4	0.3	0.4	0.2	2.2	−0.3	−3.2	0.4	1.0	3.0
Feb 1959	0.3	0.4	0.2	−0.0	0.9	1.6	−1.3	−0.5	0.9	8.6
Mar 1959	0.3	0.3	0.4	0.2	0.6	−1.8	−0.9	1.0	0.7	0.2
Apr 1959	0.4	0.3	0.3	−0.3	−0.4	−2.1	−1.5	0.4	0.1	−6.0
Year 58–59	0.1	0.1	−0.4	−0.5	1.8	−0.3	−1.5	0.1	0.6	0.8
May 1959	0.1	−0.0	−0.7	−0.7	1.2	−0.5	−2.6	−0.3	0.6	−4.6
Jun 1959	0.0	−0.2	−1.6	−1.5	0.5	−1.9	−1.5	−0.1	−0.3	−13.6
Jul 1959	0.0	−0.3	−1.9	−1.6	2.9	−0.5	−1.7	−0.8	0.2	−9.4
Aug 1959	0.0	−0.3	−1.7	−1.3	1.8	−0.9	−1.4	−0.3	0.0	−9.6
Sep 1959	0.2	−0.1	−1.3	−0.9	3.8	0.1	−0.8	0.3	1.3	4.4
Oct 1959	0.3	0.2	−0.2	−0.3	2.9	−0.9	−1.0	0.5	0.7	5.1
Nov 1959	0.5	0.4	0.5	0.1	1.2	−2.5	−2.5	−0.4	0.0	−8.2
Dec 1959	0.4	0.4	0.6	0.1	0.6	−1.0	−1.3	0.9	−0.1	−1.2
Jan 1960	0.1	0.3	0.5	0.2	1.1	−1.1	−1.0	0.2	1.0	4.0
Feb 1960	0.0	0.2	0.6	0.2	0.1	−2.0	−1.9	0.8	0.1	−1.2
Mar 1960	0.0	0.2	0.1	−0.0	−0.5	0.3	0.8	0.6	0.6	4.4
Apr 1960	0.1	0.1	0.1	−0.1	−0.4	−2.0	−2.6	0.4	−0.5	−8.0
Year 59–60	0.2	0.1	−0.4	−0.5	1.3	−1.1	−1.4	0.1	0.3	−3.2
May 1960	0.0	−0.0	−0.7	−0.5	0.3	−3.5	−1.8	−0.0	0.3	−9.3
Jun 1960	−0.2	−0.3	−1.6	−1.1	0.6	−2.3	−2.2	−0.3	0.6	−12.6
Jul 1960	−0.2	−0.4	−1.9	−0.7	2.9	−0.4	−1.2	−0.8	−0.1	−5.9
Aug 1960	−0.1	−0.4	−1.9	−1.4	3.8	0.7	−1.4	−0.5	0.8	−0.8
Sep 1960	0.1	−0.1	−1.2	−0.8	3.2	0.2	−1.8	−0.5	0.6	−1.8
Oct 1960	0.3	0.2	0.2	0.0	4.1	0.4	0.3	0.5	1.3	13.6
Nov 1960	0.2	0.2	0.2	−0.2	1.1	0.1	−1.0	0.8	1.2	4.3
Dec 1960	0.2	0.3	0.9	0.3	2.0	−2.3	−3.3	0.2	0.4	−4.2
Jan 1961	0.3	0.3	0.5	−0.1	2.1	−0.9	−1.9	0.7	0.8	2.8
Feb 1961	0.2	0.2	−0.1	−0.2	1.3	−3.1	−1.4	1.4	0.7	−3.0
Mar 1961	0.2	0.2	0.2	−0.3	1.0	0.2	−0.5	1.8	0.9	6.9
Apr 1961	0.1	0.1	−0.2	−0.5	−0.9	−2.7	−2.1	0.2	0.3	−12.8
Year 60–61	0.1	0.0	−0.5	−0.5	1.8	−1.1	−1.5	0.3	0.6	−1.9
May 1961	0.3	0.1	−0.5	−0.5	1.1	−1.0	−1.8	0.1	0.7	−2.2
Jun 1961	0.4	0.1	−0.8	−1.2	2.2	−1.3	−2.5	−0.4	−0.2	−9.6
Jul 1961	0.4	0.0	−1.0	−1.4	3.2	−1.5	−1.8	−0.3	0.3	−7.2
Aug 1961	0.4	−0.2	−1.8	−1.5	3.4	0.1	−1.6	−0.4	0.3	−4.6
Sep 1961	0.5	−0.1	−1.2	−1.1	4.0	−0.1	−1.2	−0.7	0.3	−0.8
Oct 1961	0.5	0.2	0.1	−0.4	1.7	0.2	−0.1	−0.1	−0.2	0.8
Nov 1961	0.4	0.2	0.3	0.1	1.5	−0.0	−0.3	0.4	−0.5	4.4
Dec 1961	0.0	0.1	0.3	−0.1	2.3	−0.6	−0.9	1.4	0.7	6.0
Jan 1962	0.1	0.3	0.2	−0.2	2.8	−1.6	−2.0	0.2	1.0	1.2
Feb 1962	0.3	0.2	0.0	−0.4	1.0	0.1	−1.9	−0.4	1.6	2.4
Mar 1962	0.2	0.2	0.0	−0.0	0.8	−1.0	−1.8	0.4	0.7	1.1
Apr 1962	0.3	0.1	−0.5	−0.5	1.7	−2.8	−2.3	0.8	1.4	−2.6
Year 61–62	0.3	0.1	−0.4	−0.6	2.1	−0.8	−1.5	0.1	0.5	−0.9
May 1962	0.6	0.0	−1.0	−1.1	0.8	−2.9	−2.3	−0.0	0.7	−9.8
Jun 1962	0.2	−0.3	−1.7	−1.4	2.1	−1.3	−2.2	−0.2	0.6	−8.4
Jul 1962	0.3	−0.4	−2.2	−2.1	1.4	−1.5	−1.6	−0.7	−0.0	−15.8
Aug 1962	0.3	−0.3	−1.8	−3.0	2.8	−1.1	−0.9	−0.1	0.5	−10.0
Sep 1962	0.2	−0.2	−1.3	−1.3	3.9	0.7	−1.1	0.3	0.2	2.0
Oct 1962	0.2	0.1	0.0	−1.9	2.0	−0.2	−1.1	0.7	0.4	−2.2
Nov 1962	0.3	0.2	0.3	0.4	2.0	−1.5	−1.1	0.4	0.0	1.3
Dec 1962	0.3	0.3	0.3	0.1	2.2	−1.1	−2.1	0.6	1.1	3.2
Jan 1963	0.2	0.2	0.4	0.5	2.1	−2.6	−3.7	−1.2	2.1	−3.7
Feb 1963	0.3	0.2	0.1	0.1	2.2	0.2	−1.0	1.1	1.7	8.8
Mar 1963	0.2	0.0	−0.5	−0.7	1.3	−0.1	0.2	0.2	1.0	5.0
Apr 1963	0.2	0.0	−0.0	−0.3	1.3	0.1	−2.0	0.0	0.2	0.4
Year 62–63	0.3	0.0	−0.6	−0.9	2.0	−0.9	−1.6	0.1	0.7	−2.4

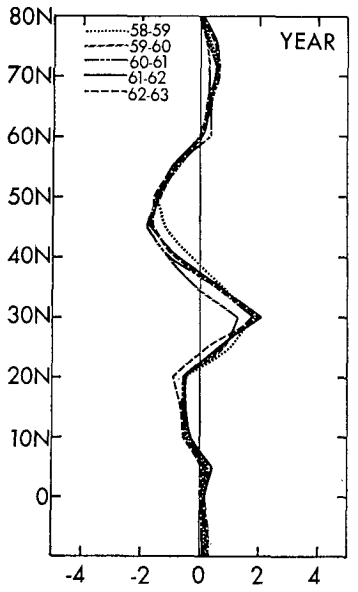

FIG. 5. Year-to-year variations (Hadleys) in the mountain torque.

However, this is not always the case. Apparently, the results are rather sensitive to both the data and the particular topography and method of calculation used. One may perhaps conclude that at any latitude the uncertainty in the evaluation of the mountain torque, because of all these effects, is of the order of 0.5 to 1 Hadley. The largest differences are found in the winter half-year. On the other hand, there is fair agreement in the larger-scale features, such as the annual-mean eastward torque around 30N, the westward torque between 40 and 60N, and the marked seasonal variations south of about 40N.

The vertical buildup given in Figs. 3 and 4 shows that the lowest three levels practically determine the value of the vertical integral, and that the latitude belt with the highest mountains, such as the one at about 35N, does not necessarily lead to the strongest mountain torque.

To supplement the midseason values discussed above, climatological mean values of the mountain torque are presented for each month of the year in Table 1. These values are based on data from the period May 1958 through April 1963. It is of interest to note the strong annual cycle south of 30N and the equally strong semiannual cycle in middle latitudes.

The hemispheric integrals in the last column of Table 1 show that on a hemispheric basis, the mountains tend to slow down the westerly circulation in summer and to somewhat strengthen it in winter. Although the quantitative differences are appreciable, Newton (1971a) obtained qualitatively the same picture with hemispheric values of +8, −5, −4 and +14 Hadleys for the months of January, April, July and October, respectively. In this connection, it may be relevant to mention the magnitude of the standard deviation in the mountain torque as computed for each calendar month from the torque values of the five individual years (see Table 2). On the average throughout the year, this standard deviation is about 4 Hadleys.

4. Year-to-year variations

In the previous section, several ways to evaluate the mountain torque were discussed and intercomparisons were made. Each method and each data set appear to have their own merits, and it is not clear that one procedure is superior to the other. Therefore, in evaluating the present year-to-year variations, the earlier results may serve as a guide to measure the uncertainty associated with the particular procedure used.

The computed values of the mountain torque for each month of the five-year period and for the five individual years are tabulated in Table 2. These values represent integrals over 5° latitude-wide belts, except in the last column where hemispheric integrals are given. The main features of the distributions are seen more readily in Figs. 5 and 6.

Fig. 5 shows, for example, that the annual-mean values of the torque do not vary much from year to year. Actually comparing Figs. 3 and 5, the interannual variations appear to be somewhat smaller than the variations due to different methods of computation. On the other hand, the curves for the same calendar month of different years in Fig. 6 show a much larger spread. With the possible exception of the winter season, the interannual differences in Fig. 6 seem to be above the level of uncertainty as suggested by Fig. 4.

During some of the months, for example March, the year-to-year differences are so large compared to the mean value that the climatological mean value for the mountain torque is not significantly different from zero. The values for August and October 1962 between 15 and 40N are questionable. However, no obvious reason could be found for the discrepancy with the results for other years.

5. Some further comments

For the general circulation of the atmosphere, the sum of the mountain and frictional torques is of most interest because it forms the net source or sink of atmospheric angular momentum. This sum averaged along a latitude circle can be computed probably most reliably in an indirect way; that is, from the atmospheric statistics themselves by integrating the horizontal convergence of angular momentum throughout the vertical extent of the atmosphere [see Eq. (1)]. However, locally the surface stress is commonly estimated from an empirical formula containing a drag coefficient and a certain power of the surface wind

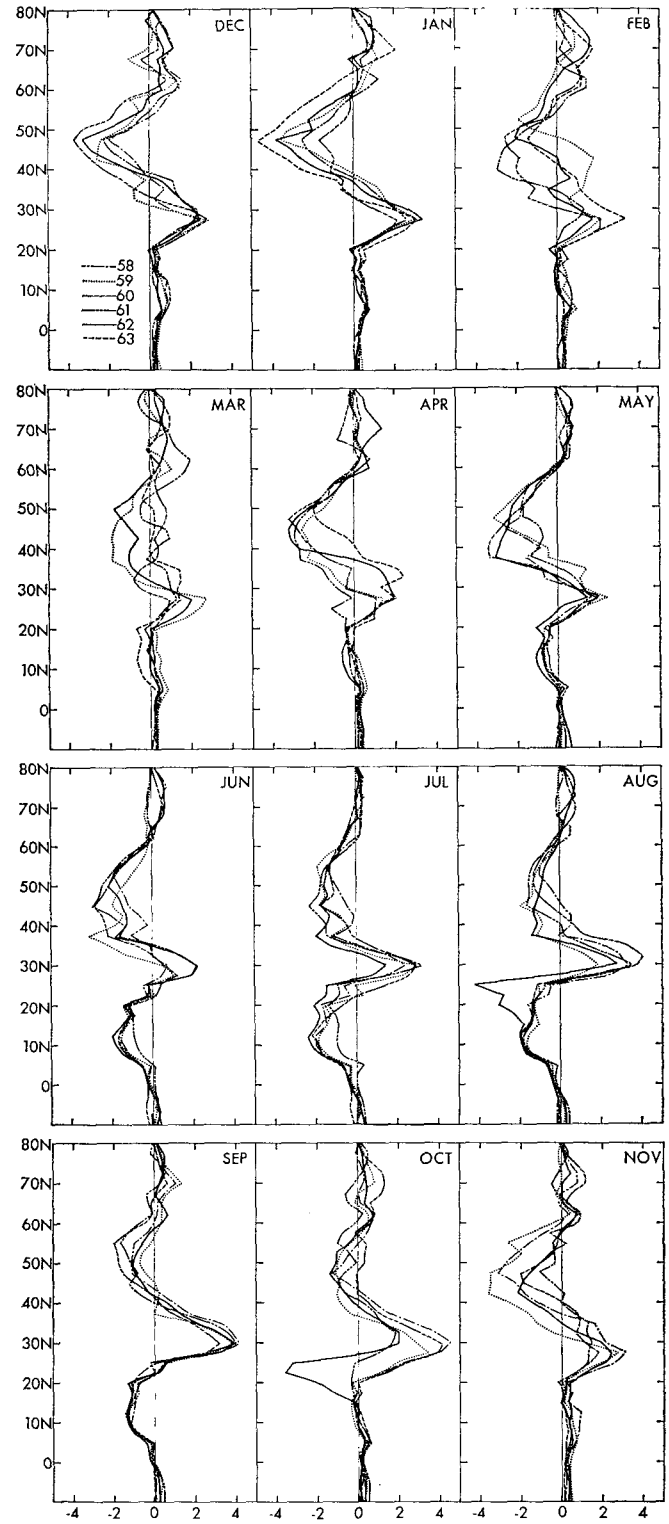

FIG. 6. Interannual variations (Hadleys) in the mountain torque for the 12 calendar months.

speed. From a summary of such earlier work by Newton (1971b), it is clear that for a particular latitude belt the large-scale mountain torque as discussed in this paper accounts generally for only a small fraction of the net surface torque.

The contribution by mountains to the *hemispheric*

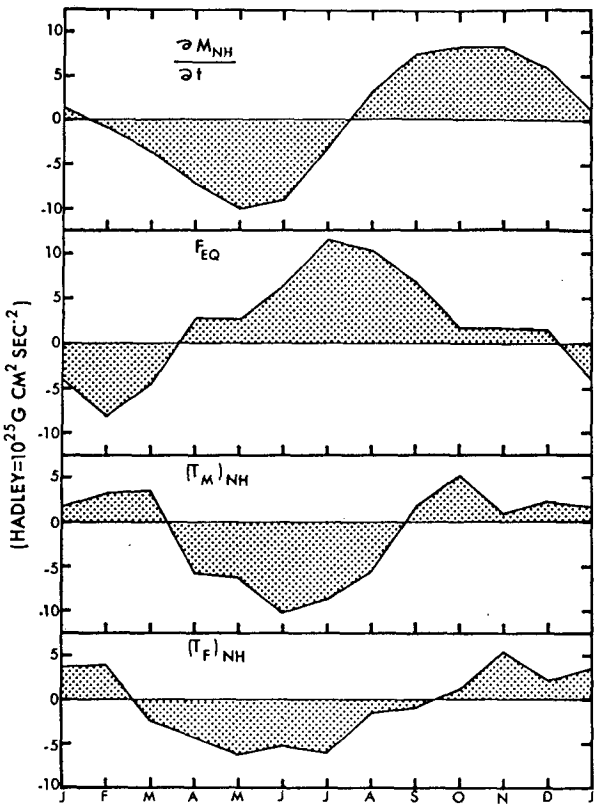

FIG. 7. Annual cycle of the different components (Hadleys) of the atmospheric angular momentum balance for the entire Northern Hemispheric mass between the surface and 75 mb.

torque is perhaps much greater. For instance, using Oort and Rasmusson's (1971) data in (1), the present authors were able to compute the rate of change of total angular momentum with time ($\partial M_{NH}/\partial t$) and the influx of angular momentum across the equatorial boundary (F_{EQ}). The surface torque $(T_M+T_F)_{NH}$ can be then derived as a residual. Finally, by subtracting the present estimates of the large-scale mountain torque $(T_M)_{NH}$ from the total surface torque, a crude estimate of the hemispheric frictional torque $(T_F)_{NH}$ was obtained. This last term includes the torque due to the unresolved mountains. The computed values are shown in Fig. 7. The first curve indicating the rate of change of hemispheric angular momentum shows, as expected, a maximum in the Northern Hemisphere fall and a minimum in the spring. The influx of angular momentum (F_{EQ}) from the Southern Hemisphere seems to be 90° out of phase with the first curve showing a maximum of inflow in July and a maximum of outflow in February as was found before by Kidson *et al.* (1969). The mountain and the residual frictional torques turn out to be of the same sign and same magnitude throughout the year. Thus, both torques appear to act on a hemispheric scale as an important sink for atmospheric angular momentum in the summer and a source in winter.

Acknowledgments. We thank Drs. H. van Loon and C. W. Newton of the National Center for Atmospheric Research for the use of their tape containing Northern Hemispheric geopotential height analyses by Crutcher and Meserve (1970). These data enabled us to make the comparison tests described in Section 3 of this paper. We are also grateful to Drs. Y. Kurihara and S. Manabe for valuable comments on the manuscript.

REFERENCES

Bretherton, F. P., 1969: Momentum transport by gravity waves. *Quart. J. Roy. Meteor. Soc.*, **95**, 213–243.

Crutcher, H. L., and J. M. Meserve, 1970: Selected level heights, temperatures and dew points for the Northern Hemisphere. NAVAIR 50-1C-52, Naval Weather Service Command, Govt. Printing Office.

Kasahara, A., T. Sasamori and W. M. Washington, 1973: Simulation experiments with a 12-layer stratospheric global circulation model. I. Dynamical effects of the earth's orography and thermal influence of continentality. *J. Atmos. Sci.*, **30**, 1229–1251.

Kidson, J. W., D. G. Vincent and R. E. Newell, 1969: Observational studies of the general circulation of the tropics: Long-term mean values. *Quart. J. Roy. Meteor. Soc.*, **95**, 258–287.

Lilly, D. K., 1972: Wave momentum flux—a GARP problem. *Bull. Amer. Meteor. Soc.*, **53**, 17–23.

Lorenz, E. N., 1951: Computations of the balance of angular momentum and the poleward transport of heat. Rept. No. 6, General Circulation Project, Dept. of Meteorology, MIT, 36 pp.

Manabe, S., and T. B. Terpstra, 1974: The effects of mountains on the general circulation of the atmosphere as identified by numerical experiments. *J. Atmos. Sci.*, **31**, 3–42.

Newton, C. W., 1971a: Mountain torques in the global angular momentum balance. *J. Atmos. Sci.*, **28**, 623–628.

——, 1971b: Global angular momentum balance: Earth torques and atmospheric fluxes. *J. Atmos. Sci.*, **28**, 1329–1341.

Oort, A. H., and E. M. Rasmusson, 1971: Atmospheric circulation statistics. NOAA Prof. Paper 5, Govt. Printing Office, 323 pp.

Starr, V. P., 1948: An essay on the general circulation of the atmosphere. *J. Meteor.*, **5**, 39–48.

White, R. M., 1949: The role of mountains in the angular momentum balance of the atmosphere. *J. Meteor.*, **6**, 353–355.

Widger, W. K., Jr., 1949: A study of the flow of angular momentum in the atmosphere. *J. Meteor.*, **6**, 291–299.